# INTEGRAL FUNCTIONS OF ELECTRON LATERAL DISTRIBUTION AND THEIR FLUCTUATIONS IN ELECTRON-PHOTON CASCADES

Ivanenko I.P., Kanevsky B.L., Kirillov A.A., Linde I.A., Lyutov Yu.G.

Institute of Nuclear Physics, Moscow State University, Moscow 119899, USSR

The paper presents Monte-Carlo simulated lateral distribution functions for electrons of EPC developing in lead, at superhigh energies (.1-1 PeV) for depths $t \lesssim 60$ c.u. $\Delta t = 1t_0$ c.u. The higher moment characteristics, i.e. variation, asymmetry, excess, are presented along with analytical solutions for the same characteristics at fixed observation level calculated to theory approximations A and B by using numerical inversion of the Laplace transformation. The conclusion is made of a complex, usually non-Gaussian shape of the function of the particle number distribution within a circle of given radius at fixed depth.

To analyse experimental data obtained by an X-ray emulsion chamber technique, the detailed information on mean EPC characteristics and their fluctuations in dense media is necessary. Therefore, in the high energy region The Landau-Pomeranchuk effect should be regarded, in the low energy region ionization losses and the Compton effect should be allowed for, and it is necessary to describe rather correctly the scattering processes. The problem being extremely complex requires the Monte-Carlo method to be used. For a simplified problem(one-dimensional theory approximations A and B, i.e. consideration of the number of particles with energy higher than the given energy), it is possible now to analyse analytically the problem of the distribution function for the particle number at fixed depth using higher moments, unlike to /1/, where only the second moment has been used. This approach allows qualitative comparison with the Monte-Carlo results and is of interest in itself as an approbation of the technique(e.g. when using the latter to analyse quark-gluon cascades).

1. A cascade from a primary of energy $E_0$ was Monte-Carlo simulated up to energies about $E=10^{-2}-10^{-3}E_0$, then each branch of 130-150 branches of the cascade was ended by statistically with a mean cascade from a previously calculated data bank. In calculations the above mentioned processes were regarded, and scattering at each segment of the free path was considered in the Fermi approximation/2/. An estimate by the method of standards assuming the initial distribution to be non-Gaussian/3/, showed that, in the range $(1/2 \div 2)t_{max}$, where $t_{max}$ is the depth of a mean shower maximum($t_{max} \gtrsim 20t_0$), a statistics of 100 events yielded an error(standard) of the mean to be 2-3%,

of variation $\sim 10\%$, of asymmetry 20-30%, and of excess 40-80%. Calculations were made on a net of 14 radii (1-400 um) given uniformly in logarithm of spatial variable, (lgr), that made it feasible to plot the differential $P(E_o,r,t)$ lateral distribution function: the particle number at distance r from the axis at depth t. The obtained differential functions were integrated and approximated.

Figs.1 and 2 compares our calculations (see the solid lines) with the experiment/4/ for the differential and integral distribution functions. The experimental results are presented for front-side film of a type C-chambers woth delution factor d=1.18 leading to a decrease of the particle number in cascade with increasing depth.

Fig.3 shows the results for 8 values of primary $\gamma$. The bundles of curves are parametrized by the product $E_oR$. The point in Fig.3 are for the results/5/. This figure illustrates violation of the core approximation of the Landau-Pomeranchuk effect. The investigation of fluctuations of the particle number within a circle of given R substantiates the general picture of evolution of the density distribution function/6/ - at $t \lesssim 1/2\ t_{max}$ and $t \gtrsim 3/2\ t_{max}$, the distributions are narrow-peaked and skewed towards the small particle number (to the left), at $1/2\ t_{max} \lesssim t \lesssim 3/2\ t_{max}$ these distributions shift to the right transforming through symmetric distributions into asymmetric ones with a flat maximum(or several maxima), Gaussian distributions in the region of $t_{max}$ are rather an exclusion than a rule. The results under consideration give a considerable qualitative clarification of the earlier data and allow investigation of the dependence on R or, what is the same, on the efficient value of threshold energy. Figs.4-6 shows $Var(E_o,t)=\sigma/m$, $As(E_o,t)=m_3/\sigma^3$, $Ex(E_o,t)=m_4/\sigma^4-3$ where $m_i=\frac{1}{n}\sum(N(E_o,R,t)-m)^i$ the numbers are for energy in TeV, R=140 um(a) and radii in um(b). The influence of the Landau-Pomeranchuk effect can be clearly seen in Fig.4 - the curve minima grows at $E_o$ 10 TeV (see Fig.4a); degrading(see Fig.4b) with increasing R corresponds to a decrease of efficient threshold energy, i.e. a weaker influence of the Landay-Pomeranchuk effect on a cascade.

2. To analyse analytically the set of equations for higher moments of the function of distribution over the particle number in approximation A, it is written in the similar form as in /1/. The solution of this set of equations can be obtained to approximation A for homogeneous cross sections and any moment using the Mellin transformation in energy $E_o$/1/. For the first, second, third etc. moments of the functions of distribution over the particle number in a shower induced by a primary electron the solutions can be represented as follows /7/:

$$\overline{Ne^1}(E_o,E,t)=\frac{1}{2\pi i}\int_{-i\infty+A}^{+i\infty+A} ds\,(E_o/E)^s\,\varphi_1(s,t)\,\frac{1}{s}$$

$$\overline{Ne^2}(E_o,E,t)=\frac{1}{(2\pi i)^2}\iint_{-i\infty+A}^{+i\infty+A} ds_1\,ds_2\left(\frac{E_o}{E}\right)^{s_1+s_2}\varphi_2(s_1,s_2,t)\,\frac{1}{s_1 s_2}$$

$$\overline{N_e^3}(E_0,E,t)=\frac{1}{(2\pi i)^3}\iiint\limits_{-i\infty+\Delta}^{+i\infty+\Delta} ds_1\,ds_2\,ds_3\left(\frac{E_0}{E}\right)^{s_1+s_2+s_3}\varphi_3(s_1,s_2,s_3)\,\frac{1}{s_1 s_2 s_3}$$

etc.

In the cascade theory approximation B similar formulae for higher moments can be obtained. These integrals for a moderate values ( $n$ =1,2,3,4) can be calculated using the numerical Laplace inversion. These calculational results are listed in Table 1 and show qualitative agreement with the simulation results. Around the shower maximum we can perform the detailed analysis of higher moments and structure of the distribution function at $E_0/E(E_0/\beta)$ . Using the saddle point method ($S_{s.p.}$ -1) it can be shown that in the region of shower maximum

$$Var \sim A_2/\sqrt{\ln E_0/E}$$

i.e. Var decreased slowly, as $\sqrt{\ln E_0/E}$, with increasing ratio $E_0/E$/8/. Asymmetry and excess increases

$$A_x \sim A_3\sqrt{\ln E_0/E}, \quad E_x \sim A_4 \ln E_0/E$$

This behaviour of higher moments contradicts the assumption of the Gaussian shape of the distribution functions for the particle number.

The investigation showed that fluctuations of the distribution functions for the particle number within a circle of fixed radius and those of the function of the number of particles with energy higher than the given energy are of similar character, oscillations of higher moments show evidence of a complex structure of the distribution functions and indicate that Gaussian distribution is rather an exclusion than a rule.


## References

1. Yanoshi L., JETP, 26, 386, 518, 1954.
   Gerasimova N.M., Trudy FIAN, 26, 192, 1964.
2. Belenky S.Z. Shower processes in cosmic rays, Gostechizdat, 243, 1948.
3. Kramer G. Mathematical methods of statistics, "Mir", Moscow, 648, 1976.
4. Hotta N. et al. Phys. Rev. D1, 22, 1, 1980.
5. Vorobyev K.V., Plyasheshnikov A.B., Uchaikin V.G., Half-analytical Monte-Carlo method. Dep. VINITI, 120, 1984.
6. Ivanenko I.P. et al. Proc. 16th ICRC, 9, 247, 1979.
7. Kanevsky B.L., Linde I.A. Proc. 17th ICRC, 6, 268, 1981,
8. Gerasimova N.M. Proc. 16th ICRC, 9, 216, 1979.


Table 1

| t | $\bar{N}$ | $Var^2$ | $A_s$ | $\bar{N}$ | $Var^2$ | $A_s$ | $\bar{N}$ | $Var^2$ | $A_s$ |
|---|---|---|---|---|---|---|---|---|---|
| 2 | 64.8 | .25 | 1.0 | 30.1 | .17 | 1.92 | .12+2 | .25 | .99 |
| 4 | 415 | .14 | .3 | 110.2 | -.11 | -.12 | .13+4 | .15 | .52 |
| 6 | 982 | .7-1 | -.45 | 157.9 | .48-1 | -1.1 | .45+4 | .94-1 | -.4-2 |
| 8 | 1333 | .31-1 | -.78 | 145 | .33-1 | -1.3 | --- | --- | -.2+1 |
| 10 | 1272 | .17-1 | -1.26 | 91.9 | .76-1 | .76-1 | .12+5 | .24-1 | -3.34 |

Table 1(continued)

| t | $\bar{N}$ | $Var^2$ | $A_s$ | $\bar{N}$ | $Var^2$ | $A_s$ | $\bar{N}$ | $Var^2$ | $A_s$ |
|---|---|---|---|---|---|---|---|---|---|
| 14 | 600 | .9-1 | .6 | 24.5 | .49 | 1.75 | .95+4 | .15-1 | .87 |
| 18 | 167 | .43-1 | .91 | 4.44 | 2.29 | 4.99 | .40+4 | .10 | 1.77 |

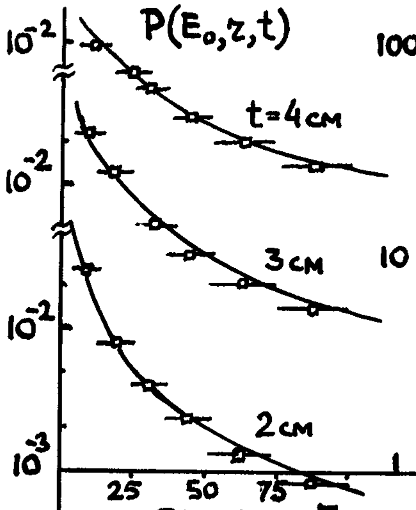


Fig.1

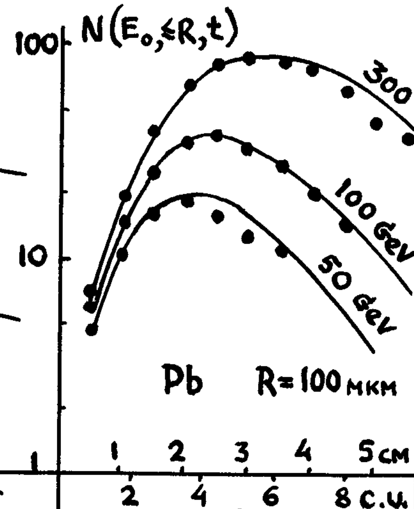


Fig.2

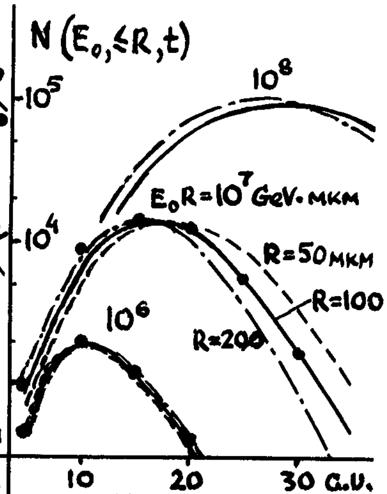


Fig.3

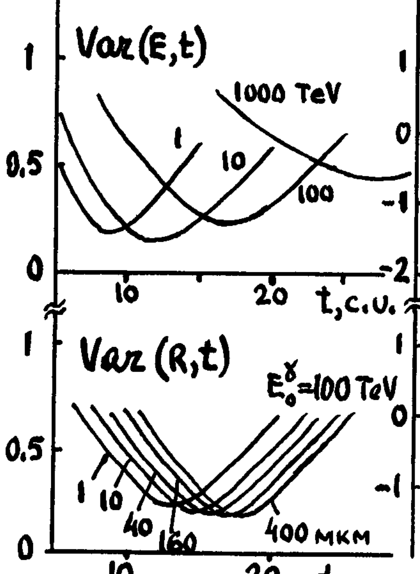


Fig.4

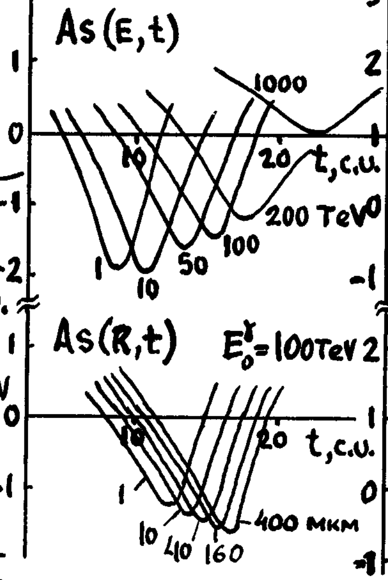


Fig.5

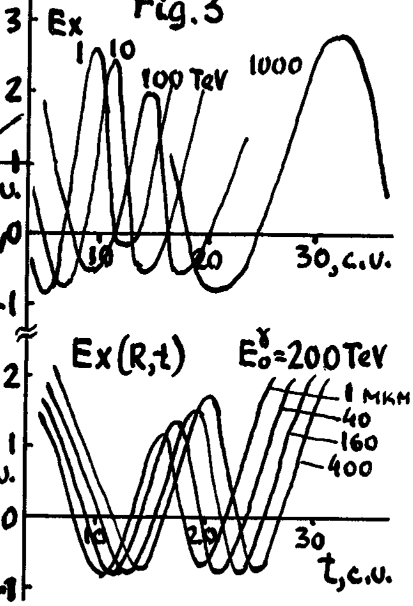


Fig.6